ENHANCING URBAN PATHFINDING FOR PEDESTRIANS THROUGH FUSION OF MLS AND HMLS DATA

S. M. González-Collazo [1], J. Balado [1], R. M. Túñez-Alcalde [1], I. Garrido [2], H. Lorenzo [1], L. Díaz-Vilariño [1]*

[1] CINTECX, Universidade de Vigo, GeoTECH Group. 36310 Vigo, Spain
(silvgonzalez, jbalado, rosamaria.tunez, hlorenzo, lucia)@uvigo.gal
[2] Defense University Center at the Spanish Naval Academy. 36920 Marín, Spain - ivgarrido@cud.uvigo.es

KEY WORDS: Deep Learning; LiDAR; navigable area; Mobile Mapping Systems; urban mobility; occlusions.

ABSTRACT: Pedestrian pathfinding is crucial for enhancing pedestrian mobility in urban environments. In this research a method to generate navigation graphs based on Mobile Laser Scanning (MLS) and Handheld Laser Scanning (HMLS) data fusion is developed. The input data comprises a 2-kilometer urban street network that integrates both MLS and HMLS data, effectively mitigating sidewalk occlusions caused mainly by parked vehicles. The proposed method encompasses the following steps: (1) Deep Learning semantic segmentation of urban ground elements and navigation-related obstacles, (2) Static vs. Dynamic object differentiation to replicate conditions of unobstructed passage. (3) Sidewalk enrichment with inclination, preservation status, and width. (4) Physical accessibility estimation between sidewalks and crosswalks incorporating curb information. And (5) navigation graph computation based on the enhanced sidewalk data, crosswalks, with accurate node location and connections. Routes were calculated within a Geographical Information System, and results ensure that pedestrians can navigate in urban environments with precision and efficiency.

1. INTRODUCTION

Pedestrian mobility is a current challenge in urban areas, with various modes of transportation such as public transport (bus, tram, train), bicycles, and walking being common choices. Across Europe, transportation preferences vary widely by country, with some favouring vehicles while others prefer cycling or walking. Percentages of people who chose walking varied between 2% and 7% being Italy and Romania the countries with the higher rates and Poland the country with the lowest one (Eurostat, 2021). Despite available navigation applications, such as Google Maps, Bing Maps, Baidu Maps, there are challenges in efficiently managing routes, particularly in considering pedestrian accessibility. Sidewalks and crosswalks are often not taken into consideration in these applications, (Balado et al., 2019). In addition, with the increase of intelligent transportation systems, pedestrians are vulnerable in traffic (Hamdani et al., 2020; K. Liu et al., 2019). Therefore, the calculation of pedestrian navigable areas in urban environments is needed to obtain safer and more accessible routes.

LiDAR technology is a valuable tool for improving mobility. Mobile Laser Scanning (MLS) technology is efficient for gathering extensive data, particularly for assessing road conditions while Handheld Mobile Laser Scanning (HMLS) provides an advantage by capturing data from the sidewalk's perspective, avoiding occlusions. However, MLS point clouds have limitations to construct navigation graphs. Point clouds are unstructured information, with noise, occlusions and strong point density variations, which must be processed in order to extract useful information (Yu et al., 2015). MLS data present occlusions in sidewalks, occurred by parked vehicles (Balado Frías et al., 2020; Barros-Ribademar et al., 2022; Z. Liu et al., 2022), which can present problems in order to obtain the navigable pedestrian space. HMLS data also present unordered points, however this data can be used to complete the occlusions in MLS sidewalk point clouds.

Graphs for pedestrian pathfinding have been generated for both indoor and outdoor spaces. In indoor environments, pathfinding primarily relies on the identification of doors and walls that delineate navigable spaces, as well as the clear floor areas without obstacles, which represent the navigable space. Flikweert et al., (2019) created an indoor navigation graph in a fast and automated way. They focused their research on door detection, being essential elements in an indoor environment. For their detection, 3D Medial Axis Transform (MAT) was used, combined with trajectory of the mobile laser scanner. (Nasir et al., 2014) studied pedestrians' routing behaviours within an indoor environment under usual situations. A network-based method using Delaunay triangulation was adopted, and a utility-based model employing dynamic programming was developed. They generated a sequence of waypoints for the pedestrian walking path using only structural definitions of the environment. Balado Frias et al., (2019) presented a methodology to enable the direct use of indoor point clouds as navigable models for pathfinding. They classified point clouds in horizontal and vertical elements according to inclination of each point respect to the neighbour. Point cloud regions classified as floor were rasterized to delimit navigable surface. A pathfinding method for an indoor drone based on a BIM-semantic model was proposed, (Chen et al., 2022). The semantic and geometric information in the BIM model was extracted and mapped to voxels to generate an indoor 3D map model called BI3DM for UAV pathfinding algorithm.

In outdoor environments, (Gaglione et al., 2022) studied a methodology for classifying a neighbourhood as more or less accessible for the elderly to reach urban services. They applied the fuzzy technique to evaluate the security and urban context characteristics. The obtained weights were then used to calculate a walking attractiveness index for the elderly using a GIS tool. Results shown the areas that local decision-makers should prioritise to improve the safety and attractiveness of routes to

* Corresponding author

access urban services. The sidewalk network of the historic city of Sabbioneta (Italy) was produced starting from point cloud data in (Treccani et al., 2022). The point cloud was semantically segmented in roads and sidewalks. They compute sidewalk attributes to generate a vector layer composed of nodes and edges with a vectorization accuracy of 98.7%. The vector layer was then used to compute accessible paths between Points of Interest, using QGIS. Balado et al., (2019) presented a methodology for the use of MLS point clouds for direct pathfinding in urban environments. They applied heuristic methods to perform semantic segmentation of point clouds and generated synthetic data to avoid occlusions. They concluded posing that the method enables the automatic generation of dense graphs representing the navigable urban space. Balado Frias et al., (2020) presented a method to obtain pedestrian navigation maps considering shadow areas and physical accessibility areas. This information was overlapped by a raster process and Dijkstra's algorithm. Accessible ways in cities were also studied in (Luaces et al., 2021) with an information system that creates an accessibility data model by ingesting different data sources: OpenStreetMap for base map, LiDAR data for geometry, volunteer information from social networks (Twitter) for accessibility problems.

Almost all the above-mentioned research used point clouds for pedestrian pathfinding and accessible routes. However, the way of dealing with point cloud limitations (occlusions, point density variations, and noise) generates very disparate navigation graphs to pedestrian mobility. Methods based on fixed nodes (located in corners, doors, etc.) imply a high dependency on identification of these geometries and oversimplify routes (loss of realism). Methods based on a grid-like distribution are not suitable for application in large urban areas, since computation time of pathfinding algorithms increases exponentially according to the number of nodes to be checked. In addition, many methods still rely on heuristic algorithms to identify navigable ground elements, or on AI algorithms limited by the number of samples. Moreover, methods using synthetic point clouds to regenerate occlusions are not faithful to reality since occlusions can hide barriers.

This study entails the fusion of point cloud data, specifically MLS and HMLS data, aimed at addressing occlusion challenges within an urban context. Urban ground elements, including the road, sidewalk, and curb, are delineated utilizing Deep Learning (DL) techniques, and their accuracy is benchmarked against heuristic approaches. Subsequently, a navigation graph is formulated, adhering to the linear layout of sidewalks while integrating critical mobility-related attributes such as accessibility, slope, preservation status and width. The practical applicability of this approach is assessed through a real-world case study, spanning a 2-kilometer urban street network, via route calculations executed within a Geographical Information System (GIS) tool.

This paper is organized as follows: Section 2 elaborates on the methodology employed in this study. Section 3 showcases the results obtained. Lastly, Section 4 concludes this work.

2. METHOD

The proposed method is based in four main steps, considering both Mobile Laser Scanning (MLS) and Handheld Mobile Laser Scanning (HMLS) point clouds as input data: 1) Semantic segmentation and occlusion correction, 2) Static/dynamic object recognition, 3) Sidewalk enrichment, 4) Graph generation for pedestrian pathfinding. Figure 1 shows the workflow.

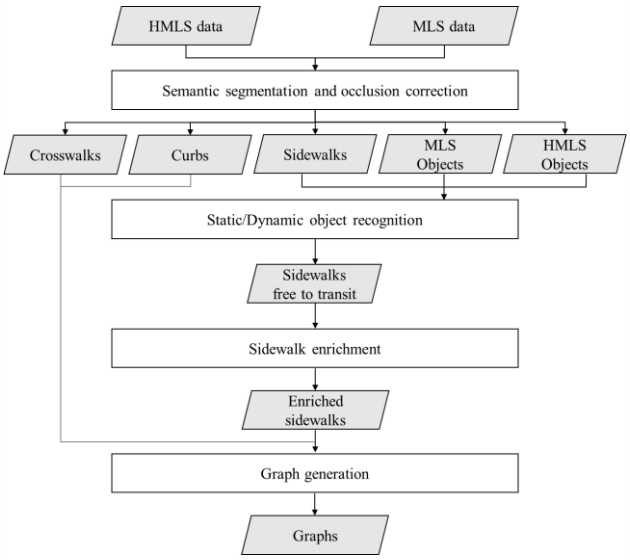

Figure 1. Workflow of the proposed method.

2.1 Semantic segmentation and occlusion correction

Point clouds are semantically segmented into navigation-relevant and comprehensive components. The initial step employs PointNet++ for the purpose of generating semantically segmented MLS and HMLS point clouds, categorized into eight classes: *road, sidewalk, curb, building, car, vegetation, pole-like* structures, and *other* entities. Subsequently, the *road, sidewalk*, and *curb* classes are isolated from the MLS dataset utilizing labeled data. Crosswalks $L_n(L_x, L_y, L_z)$ are identified within the road points, relying on their reflectivity attributes (Mi et al., 2021). Given that the MLS system operates exclusively on the road surface, the road point cloud remains unobstructed by occlusions. Conversely, the presence of parked vehicles introduces occlusions in the MLS sidewalk point cloud. To mitigate these occlusions, HMLS sidewalk point clouds are leveraged, involving a comparative analysis of distances between the HMLS and MLS sidewalk point clouds. HMLS sidewalk points that do not align within a predefined threshold distance *d* with MLS sidewalk points are retained in the final dataset.

Sidewalks, as the primary ground element for pedestrian navigation, demand improved segmentation to align with the needs of pedestrian map generation. The refinement specifically targets the removal of pavement outliers, reduction of redundant areas (from different scans), and enhancement of sidewalk individualization. The first step involves removing outlier points classified as sidewalks that hinder precise sidewalk delineation. These points are eliminated by measuring their distance from the vehicle trajectory. Points farther than a threshold *t* from the trajectory are identified as outliers and removed (see Figure 2.a and 2.b). Next, sidewalks are individualized based on MLS trajectory, resulting in a point cloud representing each sidewalk on both sides of the street (Figure 2.c). Lastly, small segments of sidewalks that have been incorrectly associated with other sidewalks are filtered out using a Density-Based Spatial Clustering of Applications with Noise (DBSCAN), (Singh & Meshram, 2017) (Figure 2.d and 2.e). Each sidewalk is then exported as a single point cloud $S_n(S_x, S_y, S_z)$.

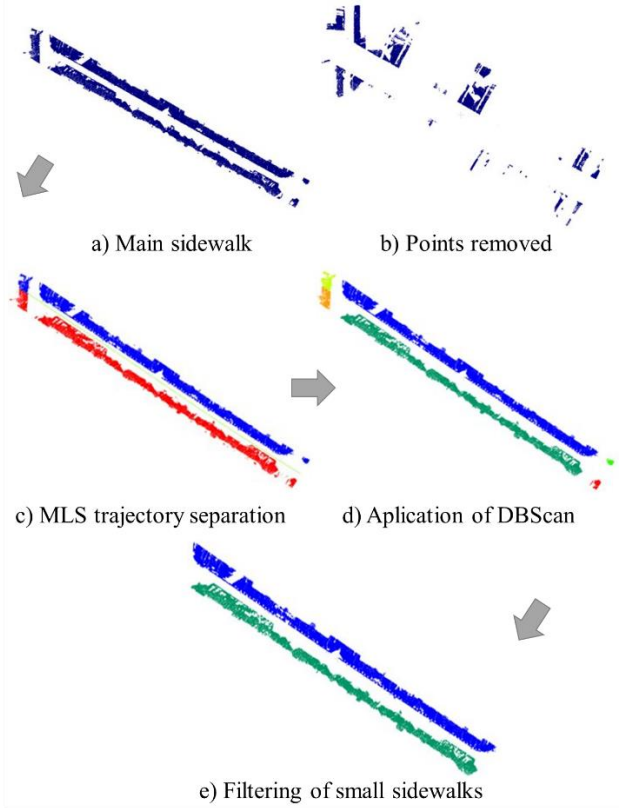

Figure 2. Sidewalk refinement

2.2 Static/dynamic object recognition

Sidewalks encompass not only fixed street furniture that can obstruct pedestrian passage, but also dynamic objects captured by MLS and HMLS that may not constitute actual obstacles. In the pursuit of generating more precise maps, a crucial step involves distinguishing between static and dynamic objects to eliminate sidewalk areas occupied by the latter.

As MLS and HMLS surveys are conducted with a temporal gap, data fusion analysis plays a pivotal role in discerning static and dynamic objects. The process commences by considering the set of points classified as objects via PointNet++, (Qi et al., 2017), (encompassing categories such as *vehicles*, *vegetation*, *poles*, and *others*). Distances between the nearest neighbours in MLS and HMLS datasets are subsequently computed. Points are categorized as static objects when the distance between MLS and HMLS points falls below a predetermined threshold *d*. Conversely, dynamic objects are identified when the distance exceeds this threshold *d*. The static objects are then subjected to individualization through the DBScan algorithm, (Singh & Meshram, 2017), and their dimensions are evaluated, considering width and height $b_W \times b_H$ factors that significantly influence pedestrian navigation in accordance with ISO-21542 (ISO, 2011).

To recreate conditions conducive to unobstructed pedestrian passage, a buffer is applied to each object. This buffer effectively results in the removal of sidewalk points located within the buffer zone, thus optimizing the representation of the sidewalk space.

2.3 Sidewalk enrichment

Three significant factors concerning pedestrian mobility on sidewalks are taken into consideration: inclination (I), preservation status (C) and width (W). The inclination (I) value is derived through the normal $N(N_X, N_Y, N_Z)$ surface estimation of the k nearest neighbours (Equation 1). In the context of preservation (C), a correlation with curvature is presumed to detect spalling and cracks, with curvature being computed from eigenvalues ($\lambda_1, \lambda_2, \lambda_3$) (Equation 2) (Weinmann et al., 2015). To establish the width, the sidewalk is segmented into cross sections following the method proposed in (Balado Frias et al., 2017). Within each cross section, W is determined as the distance between the nearest and farthest sidewalk points from the trajectory (Equation 3). As a result, each point is assigned an attribute for each feature, which is finally exported as a point cloud.

$$I = \left| atang \frac{\sqrt{N_X^2 - N_Y^2}}{N_Z} \right| \quad (1)$$

$$C = \frac{\lambda_3}{\lambda_1 + \lambda_2 + \lambda_3} \quad (2)$$

$$W = Y_{max} - Y_{min} \quad (3)$$

2.4 Graph generation for pedestrian pathfinding

The process of generating the graph relies on the selection of nodes situated on sidewalks and crosswalks, followed by the establishment of connections between these nodes and subsequent accessibility analysis. The input data for this process comprises the following components:

- Individualized sidewalks point clouds $S_n = (S_x, S_y, W, I, C)$
- Individualized crosswalks point clouds $L_n = (L_x, L_y)$
- Curb point cloud $K = (K_x, K_y)$

Sidewalk point clouds encompass pertinent information regarding the inclination (*I*), preservation status (*C*), and width (*W*) of each point. Additionally, curb data plays a crucial role in the computation of accessibility from sidewalks to crosswalks, with a particular focus on accommodating individuals with reduced mobility.

The initial step for graph generation involves the utilization of Principal Component Analysis (PCA) on the sidewalk point cloud data to ascertain the forward direction. Following this determination, a grid with a cell size *g* is superimposed along this forward direction to estimate the count of sidewalk nodes. Subsequently, the central point of each grid cell is employed to generate sidewalk nodes and associate the pertinent point cloud attributes (W, I, C) with each node.

The attributes inclination *I* and preservation *C* are assigned as the respective averages within the grid cell. As for the attribute width W, it is determined as the minimum width among the points linked to each node, signifying the most constricted pedestrian space at that point. Furthermore, two nodes are created at the boundaries of the forward direction to ensure seamless connectivity with the nearest crosswalks, thus facilitating accessibility analysis.

To handle crosswalk data, the DBScan algorithm is applied individually to each crosswalk's mark. Following this clustering, the centroid of each marking is computed, along with the calculation of the azimuth between consecutive nodes. In the final representation, each crosswalk is represented by a single

central node, and additional nodes are introduced at each extremity of the forward direction.

The connectivity between sidewalk and crosswalk nodes is established based on their proximity and alignment with the forward direction. Nodes that deviate significantly from the main direction are identified as outliers and subsequently removed from the graph to ensure the accuracy of the representation.

Finally, the physical accessibility of crosswalks is assessed based on curb information. Each entry/exit side of the crosswalks is discretized into cells with dimensions $g_c \times g_s$ in the main direction of the crosswalk and the sidewalk, respectively. The assessment is conducted by evaluating whether there are enough cells devoid of curb points to ensure the existence of a clear and unobstructed passage space in accordance with the ISO-21542 standard. If an adequate number of free cells is found, the edge corresponding to that entry/exit side of the crosswalk is marked as accessible, Figure 3. This determination contributes to the accurate representation of the physical accessibility of crosswalks in the generated graph.

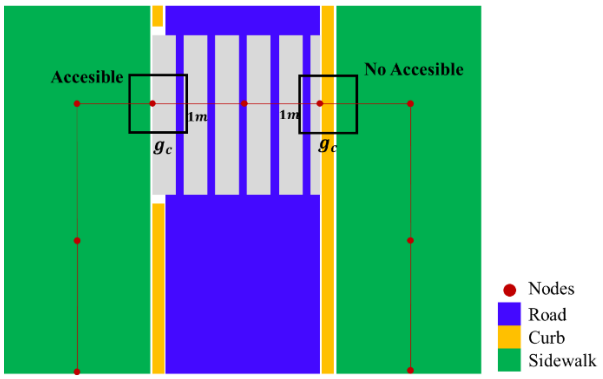

Figure 3. Accessibility analysis.

3. RESULTS

3.1 Case study

This method was tested in a 2-kilometer urban street network sited in Santiago of Compostela (Spain), which contains MLS and HMLS data. A Riegl VUX-1HA MLS scanner was used to acquire the point clouds from a car perspective and the HMLS ZEB GO scanner was also used to scan the urban environment from a pedestrian perspective. Technical characteristics are summarized in Table 1. More information of Santiago Urban Dataset (SUD) is available on (González-Collazo et al., 2024).

The proposed method was executed according to the following parameters:

- Threshold d to fusion sidewalks and detect dynamic objects was set according to MLS and HMLS point cloud registration errors.
- Threshold $t = 10$ m empirically to delimit and individualize sidewalks.
- Buffer of height $b_h = 2.2$ m and width of $b_w = 0.4$ m around static objects according to ISO-21542.
- Sidewalk width was calculated at cross sections of 1 m.
- Curvature and inclination were calculated based $k = 25$ neighbours, (Weinmann et al., 2015).
- Sidewalks nodes were obtained with a distance $g = 5\ m$.
- Each entry/exit side of the crosswalks was meshed with cells $g_c \times g_s$, being $g_c = 1\ m$ and $g_s = 10\ cm$.

	Riegl VUX-1HA	ZEB-GO
Field of view (vertical/horizontal)	360º full circle	270º/360º
Angular resolution (vertical/horizontal)	0.001º	1.8º/0.625º
Range (m)	1.2-420	30
Accuracy (mm)	5	10 - 30
Pts/s	Up to 1,000,000	43,200
Wavelength (nm)	Near infrared	905
Weight (kg)	3.75	1

Table 1. Technical characteristics of Riegl VUX-1HA and ZEB-GO

3.2 Semantic segmentation of ground elements

PointNet++ model was tested on the dataset as baseline approach. The parameters used for the pre-processing and training of PointNet++ were:

- Random cube size: 10 m per point cloud
- Random Rotation: Z axis
- Random sampling: 32768 points
- Scale data: [0,1]
- Epochs: 2000
- Batch size: 2
- Optimizer: Adam
- Learning Rate: 0.001
- Batch norm. momentum: 0.9

The quantitative results in the streets designated as test according to SUD are shown in Table 2 in comparison with algorithm published in (Balado Frias et al., 2017). The accuracies of the ground elements were very similar with both methods, however, PointNet++ errors corresponded to a noise-like error while the Balado Frias et al., (2017) errors affect entire zones thus breaking the connectivity of the navigation graph. The Balado Frias et al., (2017) algorithm could not be applied to the HMLS data because it relies on the existence of curbs to segment ground elements, while curbs were not captured from the perspective of the HMLS sensor. The processing time with (Balado Frias et al., 2017) algorithm was 12 m/min while with PointNet++ the time processing is 7 m/min, obtaining more classes.

The results from PointNet++ proved to be of sufficient quality for integration into the proposed methodology. Sidewalks were correctly completed with data from both scanners (MLS and HMLS), Figure 4.b, while curb points were obtained with some noise in the space of sidewalks, Figure 4.a.

	Road	Sidewalk	Curb	Building	Vehicles	Vegetation	Poles	Others
(Balado Frias et al., 2017) MLS	93.71%	78.79%	63.44%					
PointNet MLS	90.83%	75.58%	64.14%	94.95%	83.12%	81.19%	57.10%	23.31%
PointNet HMLS	62.20%	70.31%	0.00%	94.95%	63.91%	78.56%	61.75%	51.69%

Table 2. Accuracies using PointNet++.

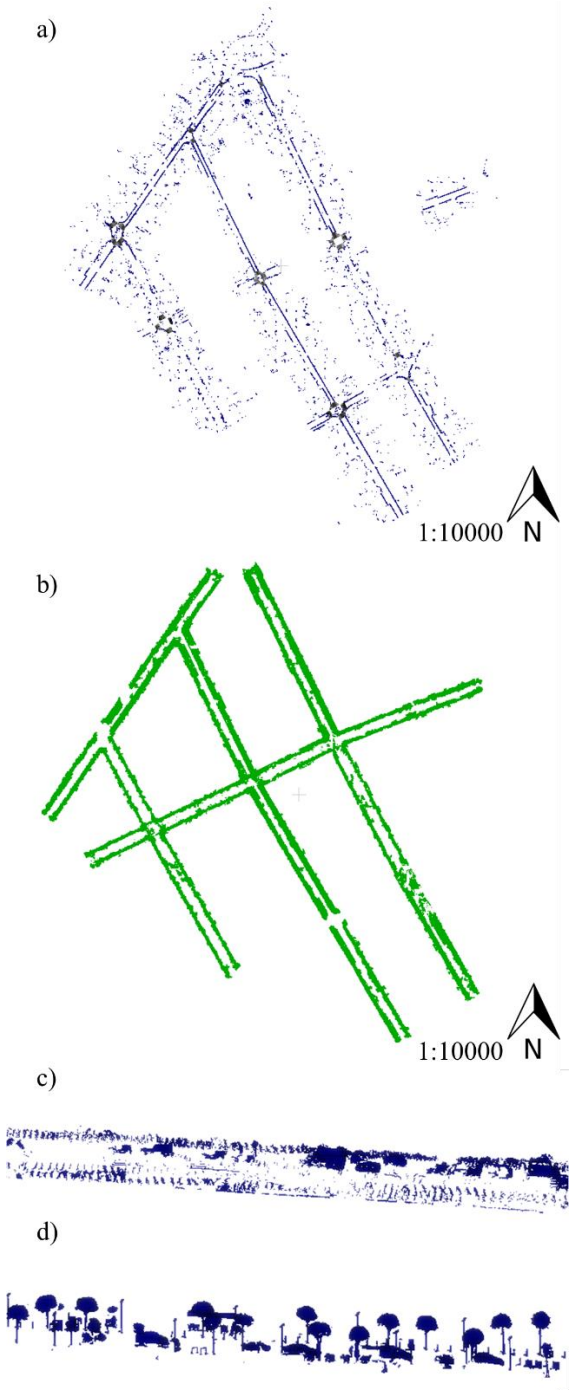

Figure 4. Semantic segmentation: a) Curbs and crosswalks, b) Sidewalks, c) Dynamic objects, d) Static objects

3.3 Dynamic and static objects

Static and dynamic elements were extracted from *vehicles*, *vegetation*, *pole-like elements* and *other* classes, computing distances between MLS and HMLS point clouds. The application of this method to the whole area may induce errors, e.g., vehicles scanned from different perspectives may be assumed to be dynamic objects. However, parked vehicles do not have influence on the navigation, due to the are not placed in the navigable space. As far as its application directly on the sidewalk is concerned, 91.6% correct detection of static objects (Figure 4.d) was obtained, and no dynamic object (Figure 4.c) was wrongly classified as static. Also, noise points were removed from static objects, being were classified as dynamic objects.

3.4 Sidewalk enrichment

Following the enrichment of the sidewalks, each segment was further subdivided into 1-meter sections for compute inclination, curvature and width values. Across almost all segments, 90% of points were within an inclination value between 0º and 15º.

Example of enriched sidewalk is shown in Figure 5. In Ramón Cabanillas Street (200 meters), most points exhibit inclinations between 0º and 6º. The sidewalks also presented low values of local curvature ranging from 0 to 0.32, indicating favourable conditions. In Frei Rosendo Salvado Street (200 meters), most points had curvature values below 0.05.

Width values were between 1.3 meters and 9.5 meters. The widest segments include points of road or building entrances, which were misclassified as sidewalks. However, such occurrences were isolated, with approximately 10 instances across the entire urban street network. The widest sections were typically found at sidewalk corners, while medium width values fall within the range of 3 to 6 meters. Fernando III Street exemplified width results.

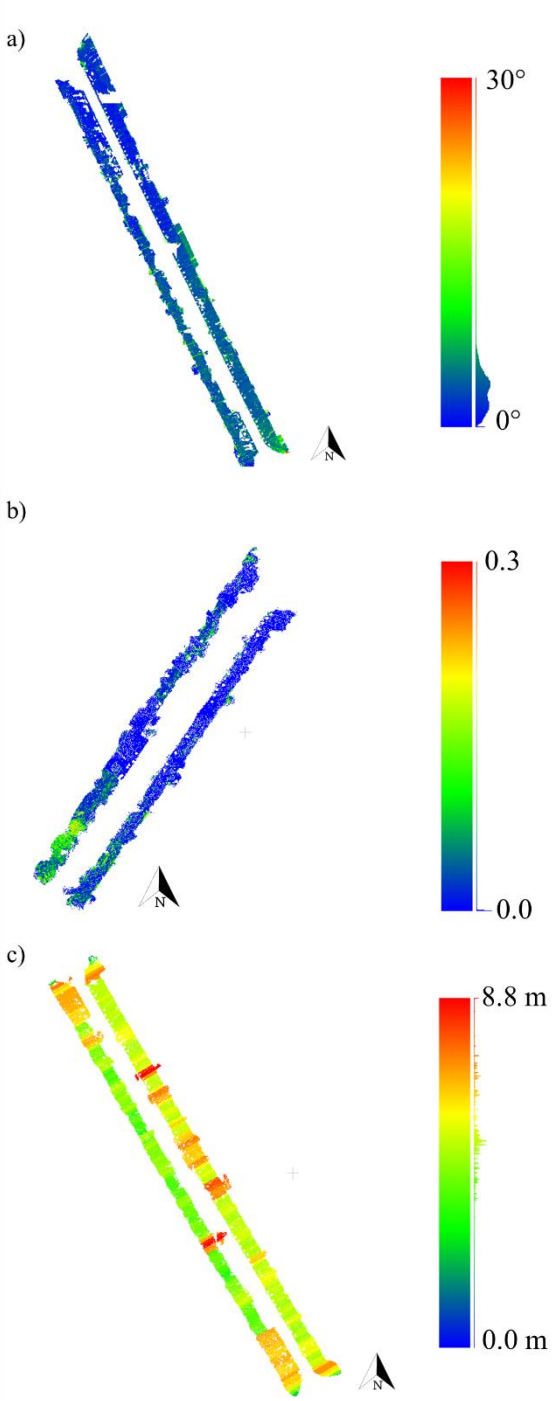

Figure 5. Sidewalk point cloud enrichment: a) Inclination in Ramón Cabanillas Street, b) Curvature in Frei Rosendo Salvado Street, c) Width in Fernando III Street.

3.5 Graphs

The graphs were visually represented by connecting lines between sequential nodes. Both nodes and lines were stored in the shapefile format. Each line contained the class (sidewalk, crosswalk or connection sidewalk-crosswalk), and physical accessibility for persons with reduced mobility. Lines connecting sidewalk nodes also included data on inclination, curvature, and width values. Accessibility values in sidewalk-crosswalks were assigned depending on the presence or absence of curbs. A value of 1 signifies accessible for persons with reduced mobility, whereas a value of 0 denotes no accessible.

The open-source software QGIS was employed for visualizing the results and conducting various tests. Given that the case study is located in Santiago de Compostela, the chosen coordinate system was ETRS89/UTM ZONE 29. The outcomes for sidewalk and crosswalk nodes are shown in Figure 6.a and Figure 6.b. The final number of nodes obtained in the pedestrian graph was 991 (835 sidewalk nodes and 156 crosswalk nodes) for the 2-kilometer urban street network.

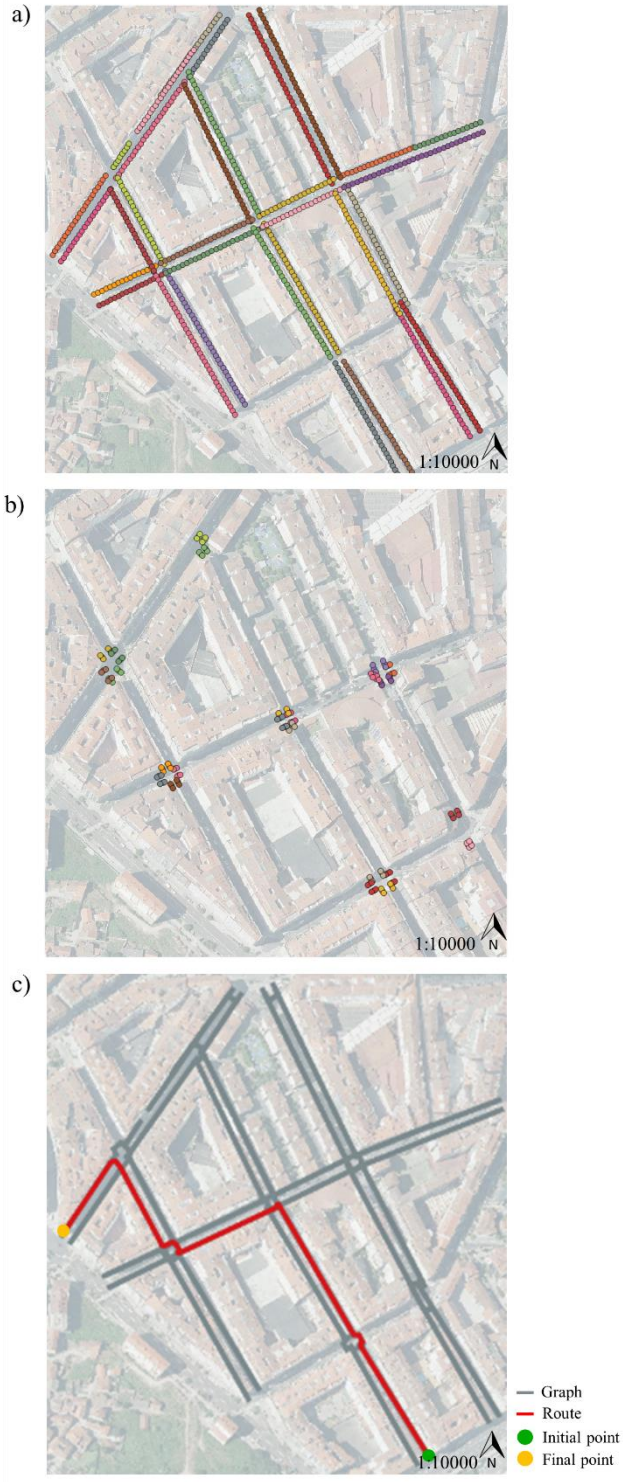

Figure 6. Graph generation: a) crosswalk nodes, b) sidewalk nodes, c) Pedestrian graph with example route

After generating the final graph, a route was computed using the Network analysis plugin in QGIS, as illustrated in Figure 6.c. An initial and final point were designated, and subsequently, the optimal route was determined based on the graph while considering the pedestrian crossings. This resulted in a route covering 625 meters, encompassing 160 nodes. The estimated time required to traverse this route was 7 minutes and 30 seconds, considering an average pedestrian speed of 5 km/h. In the method presented in (Balado et al., 2019), 140 nodes were counted within every 10 meters, while in the present method 2 nodes were represented for each 10 meters, which leads to reduce computation time.

Although several issues were addressed, it is important to note that the effectiveness of the proposed method is strongly tied to the quality of the input data. Notably, anomalies were identified during the evaluation, including a single gap within a sidewalk and four instances where sidewalk graphs erroneously overlapped with the road. These discrepancies can be largely attributed to misclassified data points when using PointNet++, emphasizing the importance of data quality and preprocessing in the graph generation process.

4. DISCUSSION AND CONCLUSIONS

This research introduces an innovative method for the precise generation of pedestrian navigation maps using MLS and HMLS point cloud data. The study employed a 2-kilometer urban street network dataset obtained from Santiago de Compostela (Spain) as input. This dataset underwent semantic segmentation via the PointNet++ algorithm, categorizing it into eight classes, which included *road*, *sidewalk*, *curb*, *building*, *vehicle*, *vegetation*, *pole-like* structures, and *other* entities. The key innovation lies in the effective utilization of both MLS and HMLS data to address sidewalk occlusions resulting from parked vehicles and to differentiate between static and dynamic objects. This differentiation significantly enhances the accuracy of pedestrian pathfinding, ensuring that navigable areas are accurately identified and represented. The method not only provides clear sidewalks free for pedestrian transit but also enriches them by calculating three essential features: inclination, the preservation status and the width.

Following the proposed method, an accurate and comprehensive pedestrian graph was successfully generated, featuring interconnected nodes representing sidewalks and crosswalks. Each node was automatically generated and annotated with its typology, and physical accessibility information. The pathfinding functionality embedded within the system enables pedestrians to effortlessly search for the shortest route by specifying their starting position and desired destination. This feature enhances the usability and practicality of the generated graph, facilitating efficient navigation for pedestrians in urban environments.

The outcomes significantly rely on the precision of the utilized DL architecture. As part of future work, alternative architectures will undergo testing, considering their respective specifications. Furthermore, the proposed method will be extended to compute public transportation graphs (bus, bike-sharing, and taxi). Additionally, there is potential for enhancing pathfinding algorithms by incorporating more characteristics (shadowy, luminosity, greenery, or other services).

ACKNOWLEDGEMENTS

This work was partially supported by human resources grant ED481B-2019-061 funded by Xunta de Galicia and RYC2020-029193-I funded by MCIN/AEI/10.13039/ 501100011033 and FSE “El FSE invierte en tu futuro”, by grant ED431F 2022/08 funded by Xunta de Galicia, Spain-GAIN, and by the projects PID2019-105221RB-C43 funded by MCIN/AEI /10.13039/501100011033 and PDC2021-121239-C32 funded by MCIN/AEI /10.13039/501100011033 and by the UE Next GenerationEU/ PRTR .The statements made herein are solely the responsibility of the authors.

REFERENCES

Balado Frias, J., Díaz Vilariño, L., Arias, P., & Frías, E. (2019). Point Clouds to Direct Indoor Pedestrian Pathfinding. *The International Archives of the Photogrammetry, Remote Sensing and Spatial Information Sciences*, *XLII-2/W13*, 753–759. https://doi.org/10.5194/isprs-archives-XLII-2-W13-753-2019

Balado Frias, J., Díaz Vilariño, L., Arias, P., & Garrido, I. (2017). Point Clouds to Indoor/Outdoor Accessibility Diagnosis. *ISPRS Annals of Photogrammetry, Remote Sensing and Spatial Information Sciences*, *IV-2/W4*, 287–293. https://doi.org/10.5194/isprs-annals-IV-2-W4-287-2017

Balado Frias, J., Díaz Vilariño, L., Frías, E., & González, E. (2020). Generation and Enrichment of Pedestrian Maps with Vertical Shadows in Urban Environments from Mobile Laser Scanning Data. *Surveying and Geospatial Engineering Journal*, *1*, 14–20. https://doi.org/10.38094/sgej114

Balado Frías, J., González Rodríguez, M. E., Verbree, E., Díaz Vilariño, L., & Lorenzo Cimadevila, H. R. (2020). *Automatic detection and characterization of ground occlusions in urban point clouds from mobile laser scanning data*. https://doi.org/10.5194/isprs-annals-VI-4-W1-2020-13-2020

Balado, J., Díaz-Vilariño, L., Arias, P., & Lorenzo, H. (2019). Point clouds for direct pedestrian pathfinding in urban environments. *ISPRS Journal of Photogrammetry and Remote Sensing*, *148*, 184–196. https://doi.org/10.1016/j.isprsjprs.2019.01.004

Barros-Ribademar, J., Balado, J., Arias, P., & González-Collazo, S. M. (2022). Visibility analysis for the occlusion detection and characterisation in street point clouds acquired with Mobile Laser Scanning. *Geocarto International*, *0*(0), 1–18. https://doi.org/10.1080/10106049.2022.2032392

Chen, Q., Chen, J., & Huang, W. (2022). Pathfinding method for an indoor drone based on a BIM-semantic model. *Advanced Engineering Informatics*, *53*, 101686. https://doi.org/10.1016/j.aei.2022.101686

Eurostat. (2021). *Passenger Mobility Statistics*. https://ec.europa.eu/eurostat/statistics-explained/index.php?title=File:Travel_distance_per_person_per_day_by_main_travel_mode_for_urban_mobility_on_all_days_(%25)_v3.png#file

Flikweert, P., Peters, R., Díaz Vilariño, L., Voûte, R., & Staats, B. (2019). Automatic Extraction of a Navigation Graph Intended for IndoorGML from an Indoor Point Cloud. *ISPRS Annals of Photogrammetry, Remote Sensing and Spatial Information Sciences*, *IV-2/W5*, 271–278. https://doi.org/10.5194/isprs-annals-IV-2-W5-271-2019

Gaglione, F., Gargiulo, C., & Zucaro, F. (2022). Where can the elderly walk? A spatial multi-criteria method to increase urban pedestrian accessibility. *Cities*, *127*, 103724. https://doi.org/10.1016/j.cities.2022.103724

González-Collazo, S. M., Balado, J., Garrido, I., Grandío, J., Rashdi, R., Tsiranidou, E., Río-Barral, P. del, Rúa, E., Puente, I., & Lorenzo, H. (2024). Santiago urban dataset SUD: Combination of Handheld and Mobile Laser Scanning point clouds. *Expert Systems with Applications*, *238*, 121842. https://doi.org/10.1016/j.eswa.2023.121842

Hamdani, S. E., Benamar, N., & Younis, M. (2020). Pedestrian Support in Intelligent Transportation Systems: Challenges, Solutions and Open issues. *Transportation Research Part C: Emerging Technologies*, *121*, 102856. https://doi.org/10.1016/j.trc.2020.102856

ISO. (2011). *ISO-21542 Building construction—Accessibility and usability of the built environment. ISO Int. Organ. Stand.*

Liu, K., Wang, W., & Wang, J. (2019). Pedestrian Detection with Lidar Point Clouds Based on Single Template Matching. *Electronics*, *8*(7). https://doi.org/10.3390/electronics8070780

Liu, Z., Oosterom, P. van, Balado, J., Swart, A., & Beers, B. (2022). Detection and reconstruction of static vehicle-related ground occlusions in point clouds from mobile laser scanning. *Automation in Construction*, *141*, 104461. https://doi.org/10.1016/j.autcon.2022.104461

Luaces, M. R., Fisteus, J. A., Sánchez-Fernández, L., Munoz-Organero, M., Balado, J., Díaz-Vilariño, L., & Lorenzo, H. (2021). Accessible Routes Integrating Data from Multiple Sources. *ISPRS International Journal of Geo-Information*, *10*(1). https://doi.org/10.3390/ijgi10010007

Nasir, M., Lim, C. P., Nahavandi, S., & Creighton, D. (2014). Prediction of pedestrians routes within a built environment in normal conditions. *Expert Systems with Applications*, *41*(10), 4975–4988. https://doi.org/10.1016/j.eswa.2014.02.034

Qi, C. R., Yi, L., Su, H., & Guibas, L. J. (2017). *PointNet++: Deep Hierarchical Feature Learning on Point Sets in a Metric Space*.

Singh, P., & Meshram, P. A. (2017). Survey of density based clustering algorithms and its variants. *2017 International Conference on Inventive Computing and Informatics (ICICI)*, 920–926. https://doi.org/10.1109/ICICI.2017.8365272

Treccani, D., Díaz-Vilariño, L., & Adami, A. (2022). Accessible Path for Historic Urban Environments: Feature Extraction and Vectorization from Point Clouds. *International Archives of the Photogrammetry, Remote Sensing and Spatial Information Sciences - ISPRS Archives*, *46*(2/W1-2022), 497–504. https://doi.org/10.5194/isprs-archives-XLVI-2-W1-2022-497-2022

Weinmann, M., Jutzi, B., Hinz, S., & Mallet, C. (2015). Semantic point cloud interpretation based on optimal neighborhoods, relevant features and efficient classifiers. *ISPRS Journal of Photogrammetry and Remote Sensing*, *105*, 286–304. https://doi.org/10.1016/j.isprsjprs.2015.01.016

Yu, Y., Li, J., Guan, H., Jia, F., & Wang, C. (2015). Learning Hierarchical Features for Automated Extraction of Road Markings From 3-D Mobile LiDAR Point Clouds. *IEEE Journal of Selected Topics in Applied Earth Observations and Remote Sensing*, *8*(2), 709–726. https://doi.org/10.1109/JSTARS.2014.2347276